Environmental Pollution 220 (2017) 95–104

Contents lists available at ScienceDirect

Environmental Pollution

journal homepage: www.elsevier.com/locate/envpol

Nonylphenol biodegradation characterizations and bacterial composition analysis of an effective consortium NP-M2☆

Naling Bai [a], Rexiding Abuduaini [a], Sheng Wang [a], Meinan Zhang [a], Xufen Zhu [b], Yuhua Zhao [a, *]

[a] Institute of Microbiology, College of Life Sciences, Zhejiang University, Hangzhou 310058, PR China
[b] Institute of Genetics, College of Life Sciences, Zhejiang University, Hangzhou 310058, PR China

ARTICLE INFO

Article history:
Received 1 June 2016
Received in revised form
8 September 2016
Accepted 11 September 2016
Available online 13 September 2016

Keywords:
Nonylphenol biodegradation
Biotoxicity assay
Co-substrates
Surface-active compound
Metabolism pathway
Bacterial composition

ABSTRACT

Nonylphenol (NP), ubiquitously detected as the degradation product of nonionic surfactants nonylphenol polyethoxylates, has been reported as an endocrine disrupter. However, most pure microorganisms can degrade only limited species of NP with low degradation efficiencies. To establish a microbial consortium that can effectively degrade different forms of NP, in this study, we isolated a facultative microbial consortium NP-M2 and characterized the biodegradation of NP by it. NP-M2 could degrade 75.61% and 89.75% of 1000 mg/L NP within 48 h and 8 days, respectively; an efficiency higher than that of any other consortium or pure microorganism reported so far. The addition of yeast extract promoted the biodegradation more significantly than that of glucose. Moreover, surface-active compounds secreted into the extracellular environment were hypothesized to promote high-efficiency metabolism of NP. The detoxification of NP by this consortium was determined. The degradation pathway was hypothesized to be initiated by oxidization of the benzene ring, followed by step-wise side-chain biodegradation. The bacterial composition of NP-M2 was determined using 16S rDNA library, and the consortium was found to mainly comprise members of the *Sphingomonas*, *Pseudomonas*, *Alicycliphilus*, and *Acidovorax* genera, with the former two accounting for 86.86% of the consortium. The high degradation efficiency of NP-M2 indicated that it could be a promising candidate for NP bioremediation in situ.

1. Introduction

Nonylphenol (NP) is a ubiquitous and stable environmental pollutant that generally originates from the biodegradation of nonylphenol polyethoxylates (NPEOs); NPEOs are primarily and widely used in industries and detergents (Krupiński et al., 2014). The increasing demand for and production of NPEOs has led to the gradual increase in NP release into the environment (Karci et al., 2014). NP can be detected in water, air, sediments, and soil, and the concentrations and half-lives vary from place to place. The predicted environmental concentrations of NP in sediments in the Wenyu River in China range from 216.8 to 8218.3 ng/g (dry weight), which is a relatively high exposure level (Zhang et al., 2015). Ieda et al. tentatively identified 102 components of NP from a technical mixture by GC × GC-MS (2005). Technical NP contained more than 20 substituted isomers having different estrogenic potencies owing to the various branching patterns of the C9 group (Preuss et al., 2006).

NP has garnered attention owing to its properties of bioaccumulation, poor bioavailability, and biological impacts including carcinogenic, teratogenic, and mutagenic effects (Krupiński et al., 2014). Generally, NP has higher estrogenicity than short-chain NPEOs, short-chain nonylphenol polyethoxy carboxylates (NPECs) (Neamţu and Frimmel, 2006), and the parental compounds (Karci et al., 2014; Wu et al., 2010). NP, as an environmental estrogen-like chemical, is capable of mimicking the actions of estrogen and interacting with human estrogen receptor, thus influencing sexual behavior and the reproductive system (Christiansen et al., 1998; Rocha et al., 2013; Shanthanagouda et al., 2013). Low concentrations of NP and octylphenol (OP) can cause malformation in the skeletal system and high concentrations can inhibit the growth of embryos (Arslan and Parlak, 2007). 4-NP at concentrations as low as 10 mg/L in water exhibits evident estrogenic potential and is absorbed through the gills and the skin (Pickford et al., 2003).

☆ This paper has been recommended for acceptance by Klaus Kummerer.
* Corresponding author.
E-mail address: yhzhao225@zju.edu.cn (Y. Zhao).

http://dx.doi.org/10.1016/j.envpol.2016.09.027
0269-7491/

Various bacterial strains have been reported to be capable of degrading NP, which are mainly affiliated to *Sphingomonas* (Corvini et al., 2004), *Stenotrophomonas* (Soares et al., 2003a), *Pseudomonas* (Fuji et al., 2000; Watanabe et al., 2012; Yuan et al., 2004), *Acidovorax* (Watanabe et al., 2012), and *Bacillus* (Chang et al., 2008). In addition, the NP-degrading ability of various fungi such as *Rhodotorula* (Wu and Qiu, 2011), *Metarhizium* (Różalska et al., 2015), and *Phanerochaete chrysosporium* (Conneely et al., 2001) has been investigated. Some researchers have also studied NP degradation and performed community analysis of river sediments (Cladiere et al., 2014; Yuan et al., 2004), bioreactors (Buitrón et al., 2015; Soares et al., 2003b), wastewater treatment plants (Press-Kristensen et al., 2008), and contaminated soils (Chang et al., 2007). NP degradation pathways are initiated by the breakdown of a phenolic moiety (Chakraborty and Dutta, 2006; Corvini et al., 2004) or by the oxidation of alkyl chains (Corti et al., 1995; Hao et al., 2010; Różalska et al., 2013). The degradation of the aromatic ring can occur in the following three ways: (1) *ipso*-hydroxylation leaving alkyl compounds as the ultimate products (De Weert et al., 2010); (2) monohydroxylation at the C atom adjacent to the hydroxyl group to produce alkylcatechol (Tuan et al., 2011); (3) dehydroxylation of the phenol ring in the initial catabolic step (Conneely et al., 2001). Importantly, most pure microorganisms were found to be effective in the degradation of only limited species of NP at low concentrations. Additionally, the degradation efficiencies of the microorganisms mentioned above were insufficient to satisfy the demand of environmental governance. In a search for microorganisms capable of degrading NP isomers with high efficiency, we isolated NP-M2 from activated sludge from a wastewater treatment plant. The metabolic pathway involved in the degradation was deduced. Our study is of great importance for the development of methods for the bioremediation of environments contaminated with NP.

2. Material and methods

2.1. Chemicals

NP (CAS 84852-15-3, MW = 220.35) was purchased from Aladdin Co. Ltd. (Shanghai, China) and used without any further purification. NP is a mixture of ring and chain isomers, with *para*-NP as the main component. Owing to its characteristics, NP does not dissolve in mineral salt medium; therefore, an individual stock solution of NP (dissolved in DMSO) was used in the culturing of the investigated bacteria.

2.2. Sampling, culture medium and cultivation techniques

The sediment samples used in this study were collected from the activated sludge from a wastewater treatment factory (Wenzhou, Zhejiang province, China). To activate the sludge bacteria, sterilized mineral salt medium (MSM) supplemented with 200 mg/L NP was used as an enrichment medium. The NP concentration was gradually increased to 1000 mg/L with continuous cultivation. Enrichment culture was continued for at least two months for successful isolation of the bacterial consortium with high NP-degrading efficiency. The sediment microcosms were incubated in flasks and incubated at 30 °C on a horizontal shaker at 200 rpm. The enrichment consortium was maintained at −80 °C in 20% (v/v) glycerol.

2.3. Growth kinetics and NP biodegradation

2.3.1. NP biodegradation in MSM

The samples investigated during the biodegradation analysis comprised 20 mL of MSM with 1000 mg/L NP as the sole carbon and energy source in each flask. The initial optical density (OD_{600}) of the bacteria inoculated in the medium was brought to 0.08. Uninoculated bottles were kept as blank controls to determine the abiotic loss of NP and incubated throughout the cultivation period. Samples were all set in triplicate for accuracy. The OD_{600} of each sample was measured daily throughout cultivation.

To study the effect of NP concentration on biodegradation performance by NP-M2, cells were cultivated in MSM with 100, 200, 500, and 1000 mg/L NP as the sole carbon source, respectively. Each treatment in different experiments was replicated three times.

2.3.2. Effects of organic substances on NP biodegradation

Glucose and yeast extract were employed as additional carbon sources during the biodegradation of NP. Glucose and yeast extract were added at different concentrations, 50 and 500 mg/L, into flasks containing 500 mg/L NP. Flasks without additional substrates (except NP) served as controls. Samples were withdrawn every 3 days to determine the different degradation efficiencies. During the period of biodegradation, the concentration of NP residues was determined using HPLC and a standard curve. The degradation efficiency (R) of the consortium was calculated as $R\ (\%) = (C_0 - C_t)/C_0 \times 100\%$, in which C_t and C_0 referred to the residual and the initial concentrations of NP at specific time periods, respectively.

2.3.3. Surface tension dynamics during NP biodegradation

An adscititious biosurfactant, rhamnolipid (RL), was employed to investigate the role of surface-active compounds. The RL used in this study, with purity more than 90%, was constituted of monorhamnolipid (Rha-$C_{10}C_{10}$) and di-rhamnolipid (Rha-Rha-$C_{10}C_{10}$). RL with 0, 0.5, and 2 CMC was added to MSM with 500 mg/L NP. Triplicated samples were collected every day to determine the concentrations of NP residues.

The dynamic change in surface tension (ST) was measured using a CAM200 tensiometer (KSV Co., Ltd.). NP/methanol (100 g/L) was weighed accurately using an electronic precision balance and filtered for use as the stock solution. The final concentration of the pollutant was brought to 1000 mg/L and methanol was completely evaporated before the experiment. MSM without NP and consortium addition was set as the blank control. Measurements were performed in a sterile atmosphere and the instrument ring was washed with sterilized distilled water.

2.4. Metabolite analysis of NP and extraction procedures

After incubation for the predetermined period at 30 °C and 200 rpm, flasks were directly fetched to extract residual NP. The samples were extracted using isometric chloroform twice under ultrasonic condition for 30 min. Next, the organic phases were collected together. The sublayer was evaporated, dissolved in 5 mL methanol, and filtered using a 0.22-μm PVDF membrane filter. The concentration of NP was measured using an HPLC apparatus as described previously (Wang et al., 2014) with some modifications. The HPLC system was equipped with an Eclipse C18 column (250 × 4.6 mm, 5 μm) (Agilent technologies, USA) and a UV detector. Methanol-water (95:5) was used as the mobile phase at a flow rate of 1 mL/min. A wavelength of 270 nm was used; the injection volume was set at 20 μL.

GC-MS analysis was adopted to determine the change curve of the residue NP and metabolite in the liquid phase. After the samples were extracted using isometric chloroform twice, the water phase was acidified to a pH of 2.0 using HCl, followed by extraction using isometric ethyl acetate. After drying by anhydrous Na_2SO_4, the intermediates were redissolved and concentrated in 5 mL of methanol. The method used for separation of NP isomers and

identification of intermediates was reported in a previous study (Tanghe et al., 2000). A 1-μL aliquot of the sample was injected into the injector in the splitless mode. The initial temperature was set at 60 °C for 1 min, followed by a 5 °C/min increment to 220 °C for 1 min. The temperature was consequently increased at a rate of 15 °C/min up to 280 °C with a 1-min hold. The temperature for the injector and transfer lines were 270 and 280 °C, respectively. The mass scan scope evaluated a range from 40 to 500 amu.

To study the key mechanism pathway in detail, we attempted to determine any volatile metabolites production. The NP-degrading consortium was cultured in glass bottles sealed with rubber stoppers and crimped. Air change was performed every 12 h to guarantee aerobic biodegradation, and 20 mL of the gas in the headspace was collected in the gas collecting bottles every day. Headspace samples were analyzed in the splitless mode using GC-MS equipped with a DB-5MS fused silica capillary column (30 m × 0.25 mm, i.d., 0.25 μm d_f) (Agilent) (Porter and Hay, 2007).

2.5. Biotoxicity assays

2.5.1. Preparation of degradation solutions

NP-M2 was cultivated in 20 mL of MSM with 1000 mg/L NP as the sole carbon source. Cultures with sterilized consortium NP-M2 in MSM were cultivated along with the treatment groups to avoid the impact of bacteria adsorption. Samples at 0, 1, 2, 4, and 6 days were sacrificed and sterilized to avoid the influence of the consortium. After centrifugation at 10,000×*g* for 10 min the suspensions can be used as the degradation solutions to do the biotoxicity assays. Cultures with 1% DMSO and without any carbohydrate were established as controls. All samples were measured in triplicate for accuracy.

2.5.2. Algal growth inhibition test

Chlorella vulgaris was cultured in BG11 medium in an illumination incubator with a temperature and humidity of 25 °C and 65%, respectively (PengFei et al., 2013). The culture was incubated under a light/dark cycle of 14 h/10 h and 60 μmol photons m^{-2} s^{-1} to simulate the actual growth condition.

The initial incubation biomass of *C. vulgaris* was measured as the chlorophyll *a* (Chla), with the value of 1.44 μg/mL. Ten milliliters of degradation solutions were mixed with *C. vulgaris* cultures. After 96-h incubation of *C. vulgaris*, the toxicity of the cultures during the degradation process was assayed by determining the Chla concentration. Chla extraction was conducted as described previously with some modifications (Sun et al., 2016). *C. vulgaris* (1 mL) was centrifuged and suspended in 0.2 mL of distilled water. After boiling at 100 °C for 3 min, the suspension was cooled to room temperature in the dark. Then, 0.8 mL of acetone was added to the solution and the mixture was centrifuged again. The OD_{665} of the upper phase was measured. The content of Chla was calculated as: ρ (Chla) (μg/mL) = OD_{665} × 13.9.

2.5.3. Phytotoxicity study

The phytotoxicity of the NP biodegradation solution was determined by a germination assay. Seeds of Chinese cabbage (*Brassica chinensis* Linn.) were sterilized in a 3% hydrogen peroxide solution for 5 min and washed with sterilized water 5 times. Thirty Chinese cabbage seeds were put into a petri dish containing 6 mL of NP degradation solution. The seeds were cultivated at 22 °C with 65% humidity, with a light/dark cycle of 12 h/12 h. Seeds cultivated in MSM without any carbon source were set as a control. Germination rate, shoot length, and root length were measured after 5 days.

2.6. Bacterial structure composition of NP-M2 and identification of functional degradation genes

The NP-M2 consortium was cultured in MSM with NP as the sole carbon source. During 8 days of cultivation, a 10-mL aliquot of culture medium was sampled every day and subjected to denaturing gradient gel electrophoresis (DGGE) analysis (He et al., 2013).

To confirm the bacterial composition of the enrichment sample, a 16S rDNA library of the consortium was constructed and sequenced. On the 4th day of incubation, genomic DNA was extracted using a genomic DNA extraction kit (TransGen Biotech, Beijing, China). 16S rDNA sequences were amplified by polymerase chain reaction (PCR). The PCR program was set as follows: predenaturation at 95 °C for 5 min, followed by 30 cycles of denaturation at 95 °C for 30 s, annealing at 55 °C for 30 s, and extension at 72 °C for 90 s, followed by a final step at 72 °C for 5 min. To avoid bias, three replications of PCR products were mixed together. Purified PCR products were ligated into a pMD19-T vector, and subsequently transformed into competent *Escherichia coli* DH5α cells. All positive clones were further cultured and sequenced by Sangon (Shanghai, China). The nucleotide sequences were used to determine species identity by comparison with sequences of known species obtained from NCBI.

Genes encoding alkane hydroxylases (ALK), catechol 1,2-dioxygenase (C12O), catechol 2,3-dioxygenase (C23O), single component monooxygenase (sMO), and multicomponent phenol hydroxylase (α-subunit) (mPH) were amplified as described in previous studies (Kloos et al., 2006; Pérez-de-Mora et al., 2011; Tuan et al., 2011; Wang et al., 2014).

2.7. Statistical analysis

Data were presented as the mean ± standard deviation (SD). Analysis of variance was performed using SPSS 16.0 software (IBM, Armonk, NY, USA).

3. Results and discussion

3.1. Consortium enrichment and NP biodegradation

A microbial consortium, NP-M2, capable of mineralizing NP as the sole carbon source, was enriched and isolated from activated sludge by continuous transferring cultivation. The growth curve and degradation ability of NP-M2 with 1000 mg/L NP as the sole carbon and energy source are shown in Fig. 1. Generally, transparent droplets of NP float on the medium owing to its lower density. During NP-M2 cultivation, the droplets tended to gradually become tawny and smaller, with no distinct micro droplets found at the end of the culture cycle. Without any evident lag phase, the NP-M2 consortium degraded 65.05% of NP on the first day. During the plateau phase, NP was continuously removed, and more than 84.69% of NP was removed in 4 days. NP degradation was limited in the next few days, which may be caused by the deterioration of the growth environment or due to bacterial die-off. After 8 days of culture, the NP-degradation efficiency reached 89.75%. In the end, along with a decrease in the amount of NP, an increase in the OD_{600} of NP-M2 to approximately 0.70 was observed. The inconspicuous reduction in NP in the control flasks was due to its volatility from the aqueous solutions. However, the significant decrease in NP concentration in the test flasks was primarily due to mineralization by NP-M2 in this study. Long-chain phenols, which act as environmental estrogens, are often detected in environment (Boitsov et al., 2007). Researches have been in full swing in the recent years in order to explore efficient NP biodegraders; however, the microorganisms studied so far can only degrade certain species of

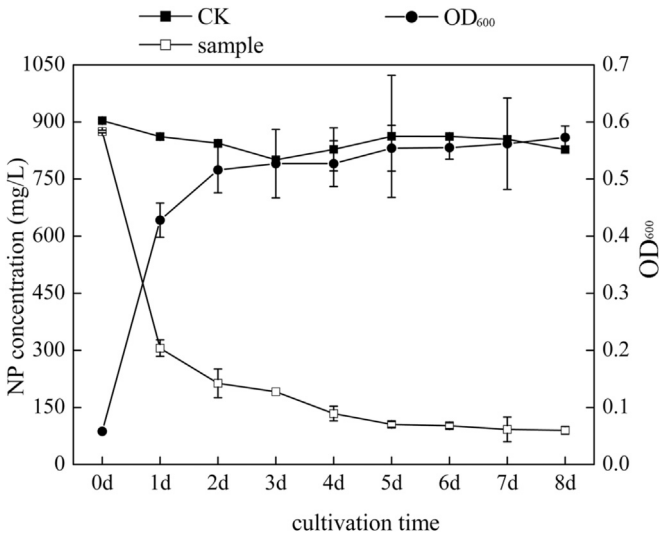

Fig. 1. Growth curve and degradation kinetics of consortium NP-M2 in MSM with 1000 mg/L NP as the sole carbon source and energy source. Dark squares: control flasks without inocula to test the effects of abiotic degradation and evaporation; white squares: NP removal by NP-M2 in 8 days; dark circles: optical density at 600 nm of NP-M2 in MSM.

NP (Janicki et al., 2016). Therefore, more effective microorganisms to degrade all NP isomers are urgently needed. The degradation efficiency of NP-M2 was higher than those observed in previous studies (Corvini et al., 2004).

The degradation products of NP at 0, 2, and 6 days were analyzed by total ion chromatography (TIC) (Fig. 2A, B, and 2C). The number of peaks detected by TIC indicated that the NP used in this study had various isomers with linear and branched alkyl chains (Corvini et al., 2004). The majority of NP isomers were removed within 2 days, while limited removal of the other NP isomers occurred in later days. As the residue concentration of NP was stable in the later days, it was hypothesized that NP isomers recalcitrant to biodegradation were detained. Therefore, the incomplete removal of NP probably resulted from the accumulation of isomers that were extremely resistant to biodegradation.

The degradation of different concentrations of NP by NP-M2 was analyzed (Fig. 3A). After a lag phase required for acclimation of only 12 h, the concentration of NP started to decrease. The degradation rate reached its maximum in the first 2 days; 61.03%, 79.60%, 54.81%, and 66.73% of NP was removed from 100, 200, 500, and 1000 mg/L NP, respectively, in 2 days. The increase in NP removal efficiency correlated with an increase in biomass (Fig. 3B). In the stationary phase, the OD_{600} showed a gradual increase, but the degradation rate of NP decreased slightly, which may be explained by further utilization of metabolites. The maximum degradation rate was 1.18, 3.25, 5.48, and 12.59 mg/L.h, for 100, 200, 500, and 1000 mg/L NP, respectively. Notably, after cultivation for 16 days, 6.45, 10.22, 31.95, and 82.17 mg/L residue was left for 100, 200, 500, and 1000 mg/L NP, respectively. NP isomers with higher bulkiness of the alpha-sub quaternary benzylic carbon atom are more estrogenic (Gabriel et al., 2005), and moreover, resistant to biodegradation (Lu et al., 2015).

3.2. Effects of additional organic substances on NP biodegradation

Co-substrates can affect the transformation or degradation of priority pollutants (He et al., 2013). Generally, extra substances play important roles in biodegradation in the environment as well as in NP removal (Chang et al., 2008; Krupiński et al., 2014); therefore, the effects of glucose and yeast extract on the degradation of NP were explored in this study. The addition of supplemental carbon at different concentrations did not decrease the degradation rate (Fig. 3C). We found that, in both samples with 500 mg/L glucose and yeast extract, the removal rate was greatly enhanced for the duration of the culture. However, 50 mg/L of glucose or yeast extract did not have any significant effect on NP degradation. Although it slightly decreased the initial degradation rate, 50 mg/L of glucose or yeast extract had no influence on the final reduction of

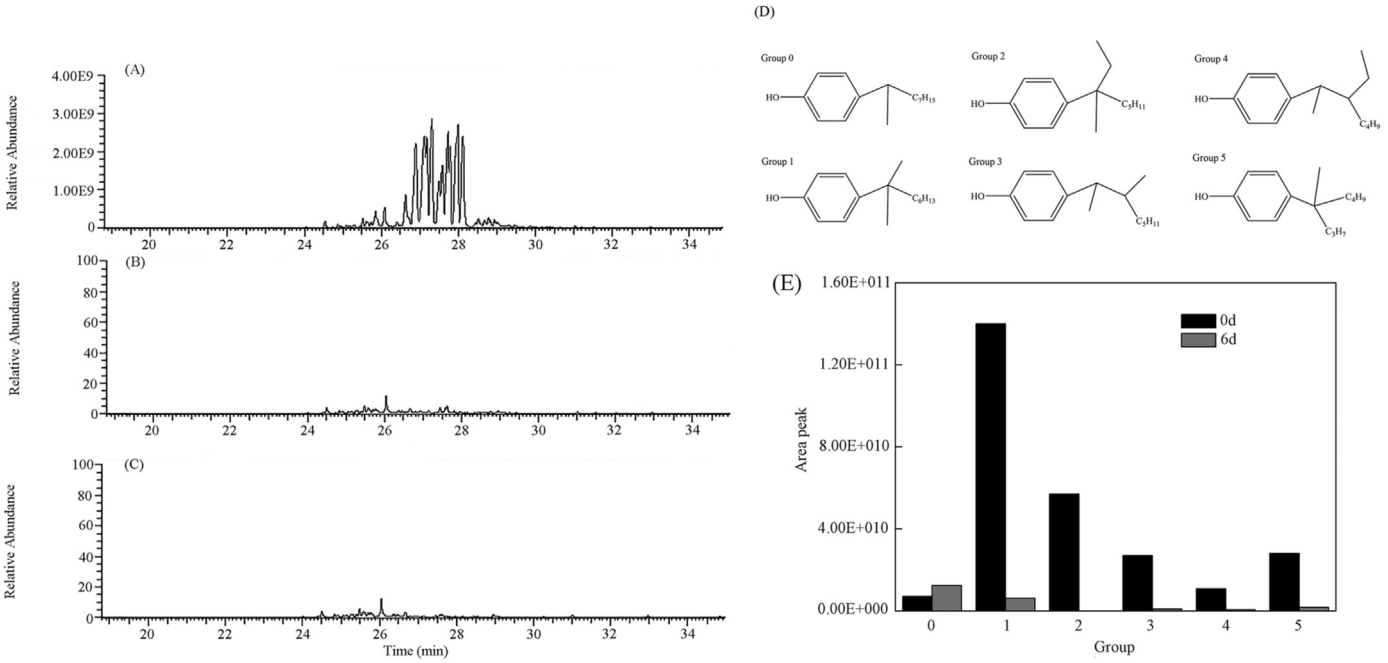

Fig. 2. (A), (B), and (C) refer to the TIC of NP biodegradation at 0, 2 and 6 days by consortium NP-M2 by GC-MS analysis, respectively; (D) NP isomer groups with different substituent configurations; (E) Degradation of specific groups of NP isomers by NP-M2 after 6 days of cultivation.

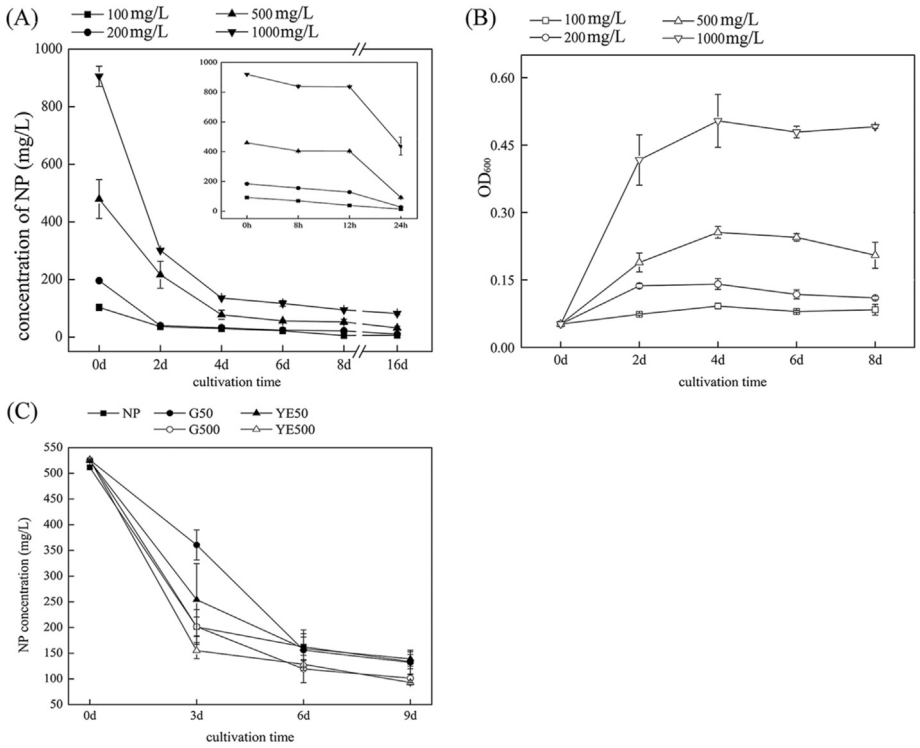

Fig. 3. (A) Biodegradation of different concentrations of NP by NP-M2; (B) Growth curve of NP-M2 in presence of different dose of NP; (C) Effects of additional substrates on NP biodegradation (initial NP concentration: 500 mg/L). NP: only NP as the sole carbon source and energy source. G50: additional 50 mg/L glucose; G500: additional 500 mg/L glucose; YE50: additional 50 mg/L yeast extract; YE500: additional 500 mg/L yeast extract. Error bars represent the SDs.

NP as compared to controls without additional substrates. This phenomenon might have resulted from the tendency of microorganisms to utilize bio-available materials rather than refractory pollutants. In a previous study, the addition of 20 mg/L hampered the degradation as the glucose competed with NP as the substrate (Wang et al., 2015a). However, once the expression of the relevant degradation genes was induced, the substance was metabolized rapidly. When 500 mg/L carbohydrate was added, the cells grew fast, which promoted NP degradation. When the co-substrate was added in higher doses, 24.09–30.38% more NP was removed than in the control flasks. Besides, the accelerating effect of yeast extract was more significant than that of glucose on the 3rd day, with higher degradation rate and efficiency, which was similar to that reported for the disposal of $NPEO_{av2.0}$ (Liu et al., 2006). After 3 days, the degradation rate and efficiency remained similar in both cases.

3.3. Surface tension analysis

Biodegradation is typically hampered by actual bioavailability owing to the low hydrophilicity of pollutants. The water solubility of NP was estimated to be low, ranging from 5.4 mg/L to 7.0 mg/L, which possibly affects its mobility, microbial accessibility, and degradation in the environment (Brix et al., 2001). The degradation could be successfully accelerated by solubilizing chemicals in the aqueous phase and by increasing the bioavailability of pollutant within the surfactant micelles (Zhang et al., 1997). Previous studies have focused on the effect of biosurfactants on alkanes, crude oil, and PAHs (Das et al., 2008). However, little is known about the relationship between biosurfactant secretion and NP biodegradation. The only related reported was that the surface-active action exerted by *para*-NP induced *Candida maltose* transition in the culture, thus facilitating the alkylphenol degradation (Corti et al., 1995). Emulsification was observed during initial-phase NP biodegradation. Therefore, we investigated the possible production of a surface-active compound during cultivation of NP-M2.

The result showed that the variation in ST corresponded to the NP degradation efficiency of NP-M2 and to OD_{600} (Fig. 4A). During the first 2 days, the bacteria showed fast log-phase growth, almost at the maximum value, and only 24.39% NP was remained in the culture; the ST was reduced to a minimum of 64.06 mN/m. Then, ST slowly increased back to the original value at the end of the culture period. It has been hypothesized that surface-active compounds are secreted into the extracellular environment (Deziel et al., 1996), which may have increased the concentration of NP in the aqueous solution. Therefore, we hypothesized that surface-active compounds might be produced during NP biodegradation, facilitating hydrophobic hydrocarbon removal.

Furthermore, RL was added to determine the role of surface-active compounds in NP reduction in the initial 2 days of culture, since NP was dramatically decreased in this period. As shown in Fig. 4B, the addition of RL at 0.5 or 1 CMC only slightly accelerated NP removal ($p > 0.1$). It was hypothesized that the solubilization effect of surface-active compounds excreted by NP-M2 could meet the requirement of NP concentration in aqueous phase for optimum degradation. However, high concentrations of RL hampered the degradation in the first day ($p < 0.1$), which could be explained by that excess RL may serve as a primary substrate in competition with NP or may exhibit antimicrobial activity on the cells (Whang et al., 2009). Singh et al. (2007) also noted that the addition of surfactant could either accelerate or sometimes inhibit the bioremediation of pollutants. The micellar pollutant may have variable bioavailability and thus influence the biodegradation rate, which is dependent upon the concentration of surfactant used (Zhang et al., 1997). On the other hand, high concentrations of RL slightly facilitated degradation in the second day ($p > 0.05$), which may be because RL acted as a co-substrate, thus increasing the biomass.

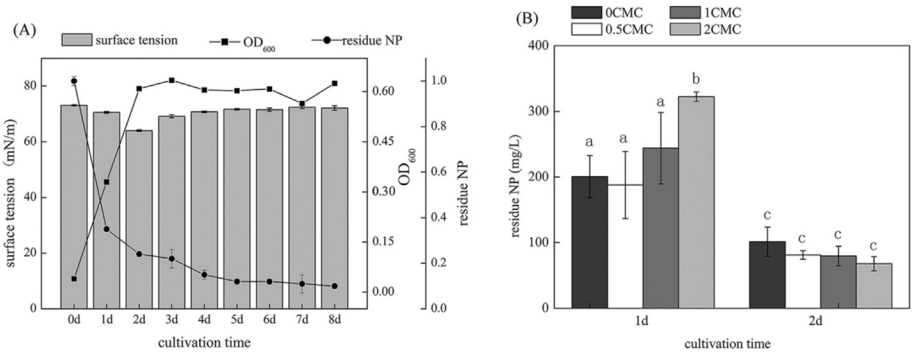

Fig. 4. (A) Changes in the growth and surface tension of NP-M2 during NP biodegradation. Black square: optical density at 600 nm of NP-M2. Black circle: ratio of residue NP in MSM. Data are expressed as the means ± SD of triplicate experiments; (B) Effect of different concentrations of RL on NP biodegradation. Different lowercase letters above the columns represent statistical significance by ANOVA analysis ($p < 0.05$).

3.4. Analysis of the intermediate produced during NP biodegradation by NP-M2

The aromatic fraction of NP was monitored using HPLC-UV, but apart from NP, no aromatic compounds were detected in the cultures during the NP degradation process. Therefore, the intermediates in the headspace and the aqueous phase were analyzed using GC-MS (Fig. 5A and B). As shown in Fig. 5C, the metabolite in the aqueous phase started increasing at day 1 and reached its maximum at day 3; soon afterwards, it decreased along with cultivation time. The metabolite had a retention time of approximately 8 min and additional fragments at *m/z* 59 (M-C_6H_{13}), 73 (M-C_5H_{11}), and 129 (M-CH_3). The mass spectra were compared with the retrieval database and a previous report (Porter and Hay, 2007), which indicated the metabolite to be nonanol. Therefore, nonanol was expected to be a major degradation product and was further metabolized. The volatile metabolites showed one distinct peak at a retention time of 6.0 min. The mass spectrum showed several significant peaks at *m/z* 55 (M-C_5H_{11}), 69 (M-C_4H_9), 84 (M-C_3H_7), and 97 (M-C_2H_5), which corresponded to nonene (Porter and Hay, 2007). The relative peak area of the nonene in the headspace also decreased with time (Fig. 5C). In previous reports, nonanols were detected both in the culture medium and the gas phase (Fuji et al., 2000), and the concentration of alcohol was much lower than that of alkene (Porter and Hay, 2007). Moreover, NP-M2 consortium was capable of degrading other substances such as isopentanol, hexanol, and nonanoic acid (data not shown). Therefore, we assumed that, unlike in the case of *Sphingomonas* sp. TTNP3 (Corvini et al., 2004), the absence of alcohols in the gas phase was due to gradual, complete biodegradation. Hydroquinone (HQ) is formed as a result of the reaction catalyzed by sMO (Corvini et al., 2006) and might be degraded instantaneously by other enzymes with short lag time. As a result, no aromatic compounds other than NP were determined, which indicated that the close cooperation among the effective microorganisms in the NP-M2 consortium accelerated the elimination of toxic compounds.

The degradation pattern of NP isomers was estimated by GC-MS analysis. Examination of the spectra indicated six distinct groups of NP isomers (Ieda et al., 2005; Lu and Gan, 2014; Wheeler et al., 1997) (Fig. 2D). The mass spectra showed a fragment ion of *m/z* 107 that was common to all nonylphenols (Fig. S1), and was therefore not discussed in the prediction of the isomers classification (Wheeler et al., 1997). Group 0 had a base peak at *m/z* 121, with no other distinct peaks in the range of 122–219, indicating a methyl group on the α-carbon. However, a relatively detailed structure could not be obtained. Group 1 had a base peak of *m/z* 135, which probably indicated an α-dimethyl structure. Some isomers had no major peaks other than the base peak, whereas the remaining

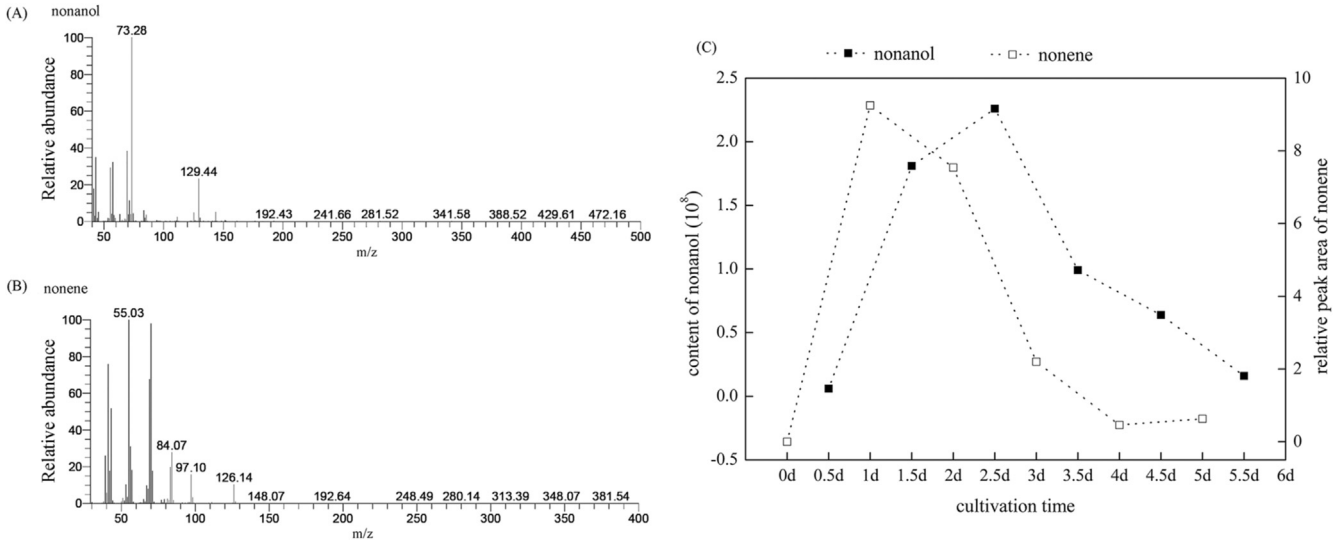

Fig. 5. Mass spectra of nonanol (A) and nonene (B); (C) The content of nonanol in the aqueous phase and the relative peak area of nonene in the gas phase.

Table 1
Treatment solutions used in this study.

	CK_{MSM}	CK_{DMSO}	0 d	1 d	2 d	4 d	6 d	Control groups			
								CK-1d	CK-2d	CK-4d	CK-6d
Bacteria	−	−	+	+	+	+	+	−	−	−	−
DMSO	−	+	+	+	+	+	+	+	+	+	+
NP	−	−	+	+	+	+	+	+	+	+	+

"+" indicates the addition of the specific substance into the MSM; "−" indicates culture in the absence of the specific substance in the MSM.

isomers contained the fragment *m/z* 149, 163, 177, or 191, suggesting a tertiary β-carbon. Group 2 isomers had methyl and ethyl substituents at the α-position, with a base peak of *m/z* 149 and a major fragment of *m/z* 191. The *m/z* 149 ions suggested the loss of C_5H_{11}, and the presence of an ethyl substituent on the α-carbon allowed the formation of the fragment ion *m/z* 191. Group 3 isomers only had significant peaks at *m/z* 121, 149, and 220; thus, it was proposed that α-methyl-β-methyl structures were present in the isomers. The three main peaks were attributed to the cleavage of α-carbon, β-carbon, and the molecular mass of NP, respectively. Group 4 isomers had a base peak of *m/z* 163 with a major peak of *m/z* 121, suggesting an α-methyl-β-ethyl substituent. The formation of *m/z* 121 indicated an α-methyl structure, and *m/z* 163 resulted from the loss of C_4H_9 from the β-carbon. Group 5 isomers had α-methyl, α-propyl, and α-butyl structures, with peaks of *m/z* 121, 163, and 177. The presence of *m/z* 163 indicated bond cleavage between the α- and β-carbons. Moreover, the loss of propyl would result in the formation of *m/z* 177. The isomers showed a sharp decrease after biodegradation (6 days) by NP-M2 to differing degrees, except for the group 0 isomers ($p < 0.05$) (Fig. 2E). The amounts of Groups 1–5 were decreased by 94–100%, and Group 2 isomers had the highest degradation efficiency. It has been reported that isomers with less bulky α-substituents are more easily degraded and have shorter half-lives (Lu and Gan, 2014). Additionally, the present results indicated that isomers with α-dimethyl (Group 1) and α-ethyl-α-methyl (Group 2) had better biodegradability, consistent with a previous report (Lu and Gan, 2014). Actually, Group 1 consisted of 57.88% of the NP as the substrate (data not shown). Notably, Group 0 isomers were only slightly degraded, possibly as a result of other steric effects; this phenomenon requires further elucidation.

3.5. Biotoxicity analysis

3.5.1. Toxicity analysis to C. vulgaris

NP can potentially harm non-target aquatic organisms. Therefore, we chose the green alga *C. vulgaris* to evaluate the ecotoxicity of NP on account of its position in the trophic chain in the aquatic ecosystem. The different conditions of the degradation solutions used are listed in Table 1. As shown in Fig. 6, 1% DMSO did not influence the growth of *C. vulgaris*. Compared to the control groups at 1, 2, 4, and 6 days, the green alga grew well in the cultures in which NP had been treated by consortium NP-M2 ($p < 0.05$). These findings suggested that the high dose of NP used had harmful effects on the alga growth. In conclusion, the dramatic detoxification performance of NP-M2 indicates its potential role in NP bioremediation in situ.

3.5.2. Phytotoxicity analysis

It is known that contaminated water can harm the environment, while treated water and sediment can be used in agriculture. Therefore, we determined the change in phytotoxicity during NP biodegradation. NP was toxic to Chinese cabbage and inhibited the growth of cabbage shoots and roots (Fig. 7). The results of the phytotoxicity assay are shown in Table 2. In untreated NP solution, the shoot and root lengths were only 0.1–0.5 cm and 0.2–0.7 cm, respectively. In contrast, in the treated groups, they both were approximately 1.0 cm. The extent of germination in the solutions at 1, 2, 4, and 6 days was not significantly different from that in MSM ($p > 0.1$). However, the germination at 0 days of treatment was low ($p < 0.1$). These results indicate that the toxicity of NP to Chinese cabbage seeds was almost totally eliminated within several days. Therefore, NP-M2 showed good detoxification of NP.

3.6. Characteristics of the NP-degrading genes

The *sMO* and *mPH* genes were detected in the consortium NP-M2, with 99% and 93% sequence identities to the octylphenol 4-monooxygenase gene of *Sphingobium xenophgam* and phenol 2-monooxygenase gene of *Alicycliphilus denitrificans*, respectively. sMO is involved in type II *ipso*-substitution of OP with HQ and branched alcohols as the metabolites (Corvini et al., 2004), which has mainly been reported in a few species of *Sphingomonas*. Most of the reported microorganisms preferentially degrade short- or medium-chain alkylphenols using *ortho*-substitution (Tuan et al., 2011). mPH can monohydroxylate the C-atom at the position adjacent to the pre-existing hydroxyl group to produce alcohols and catechols in short- and/or medium-chain alkylphenols. The aromatics are then further cleaved by either C12O or C23O (Tuan

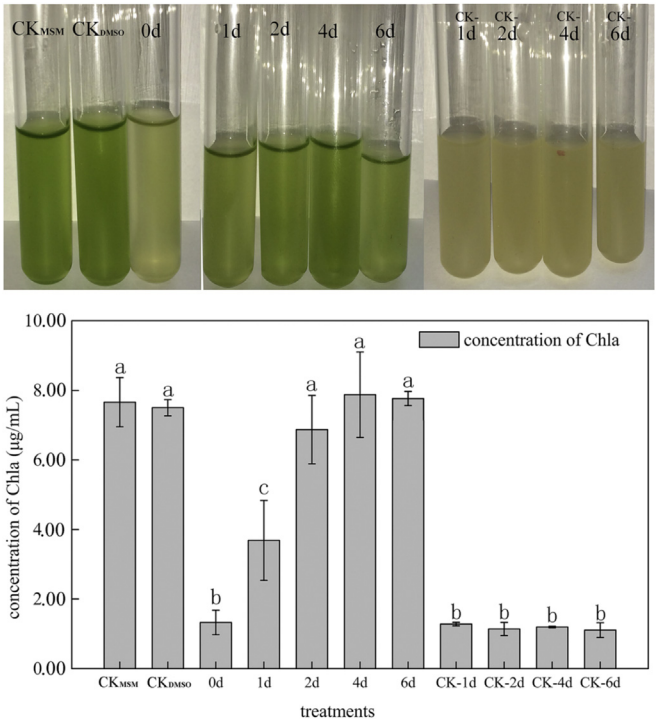

Fig. 6. Chla concentration in *C. vulgaris* after cultivation for 96 h in different solutions. The mean difference is significant at the 0.05 level.

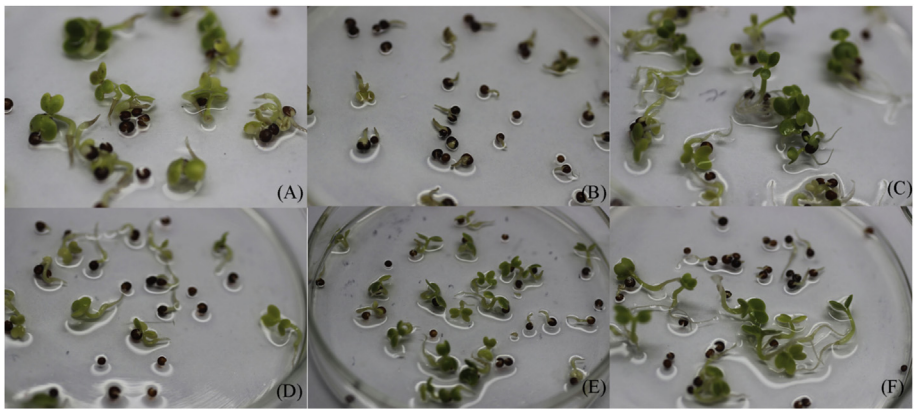

Fig. 7. Growth states of cabbage seeds after cultivation for 5 days using different solutions. The codes (A to F) in the picture refer to CK_{MSM}, 0, 1, 2, 4, and 6 days, respectively.

Table 2
Phytotoxicity of NP towards cabbage seeds.

	Chinese cabbage					
	CK_{MSM}	0 d	1 d	2 d	4 d	6 d
Germination rate (%)	85 ± 4^{a}	68 ± 13^{b}	81 ± 10^{ab}	80 ± 3^{ab}	73 ± 7^{ab}	74 ± 5^{ab}
Shoot length (cm)	1.00 ± 0.17^{a}	0.60 ± 0.14^{b}	1.27 ± 0.40^{a}	1.27 ± 0.06^{a}	1.10 ± 0.10^{a}	1.27 ± 0.12^{a}
Root length (cm)	0.70 ± 0.10^{a}	0.45 ± 0.07^{a}	1.70 ± 0.89^{b}	1.03 ± 0.12^{ab}	0.97 ± 0.32^{ab}	1.77 ± 0.93^{b}

Data are the means of triplicate experiment ± SE. Different lowercase letters are statistically different at significance level of $p < 0.1$.

et al., 2011).

In this study, a BLAST of the *C12O* gene revealed 93% sequence identity with the coding sequence of catechol 1, 2- dioxygenase of *Pseudomonas knackmussii* B13. However, the reported *C23O* gene was not amplified from the genome. Therefore, NP-M2 may not contain *C23O* genes or possesses novel catabolic enzymes genes for this step (Tuan et al., 2011). mPH, C12O, and C23O, involved in alkylphenol degradation, were identified in *Pseudomonas* sp. TX1, which can degrade both OPEO/NPEO and NP/OP (Huang et al., 2014).

The primers used in this study failed to amplify the genes involved in alkane degradation (Table 3). Therefore, additional primers were designed based on the conserved domains of different groups of alkane hydroxylase genes. Wang et al. (2014) reported the presence of the *ALK* and *C23O* genes in a linear 4-NP-degrading *Sphingobium* strain. Genes coding the enzymes for n-alkane degradation were not detected in this consortium. Furthermore, only diffuse bands could be observed with the degenerate primers ALK-F/ALK-R, even after optimizing the PCR program. This was likely due to the fact that these primers were all designed for unbranched n-alkanes. The decrease in alcohol concentration suggested that the alkyl chains were gradually metabolized. Thus, NP metabolism might be initiated by oxidation of the benzene ring, followed by degradation of the intermediates (Fig. 8).

3.7. 16S rDNA library analysis

Samples were withdrawn every day during 8 days of incubation to analyze the community structure changes during NP biodegradation. The composition of the NP-M2 consortium was stable during NP degradation, as determined by DGGE analysis (Fig. 9A). To identify the primary degraders in this stable consortium, a 16S rDNA library was constructed using the TA clone and then sequenced. *Sphingomonas* and *Pseudomonas* species made up 71.53% and 15.33% of the NP-M2 consortium, respectively (Fig. 9B). *Acidovorax* and *Alicycliphilus* species accounted for 9.49% of the consortium. These data were consistent with previous reports that proteobacteria play important roles in the biodegradation of pollutants (Viñas et al., 2005; Wang et al., 2015b). Furthermore,

Table 3
PCR detection of the functional genes in community NP-M2.

Gene	*sMO*	*mPH*	*C12O*	*C23O*	*alkB*	*alkM*	*alkB1*	*ALK*
PCR reaction	+	+	+	−	−	−	−	−

"+": positive PCR reaction; "−": negative PCR reaction.

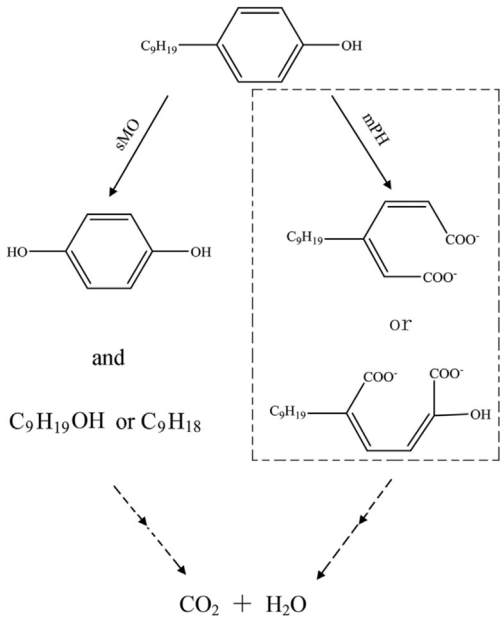

Fig. 8. Proposed NP pathway of degradation by consortium NP-M2. Dashed line: compound or reactions supposed to be present during the biodegradation.

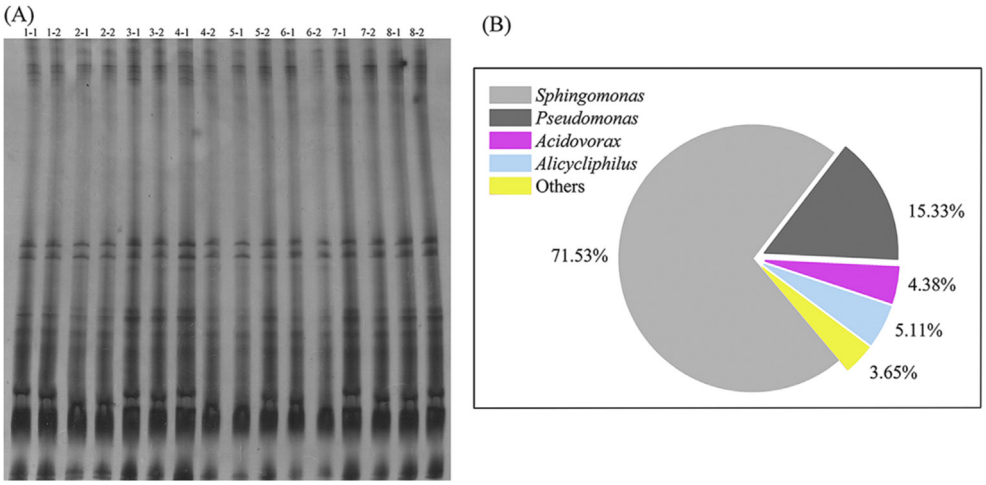

Fig. 9. (A) Microbial community structure analysis of NP-M2 during the 8 days of NP biodegradation by DGGE; (B) Bacterial composition of the NP-M2 consortium determined by 16S rDNA library analysis.

Sphingomonas, *Pseudomonas*, and *Acidovorax* species have been reported to be involved in the removal of alkylphenols and alkylphenol polyethoxylates in a series of environmental conditions. However, to our knowledge, this is the first report of the involvement of the *Alicycliphilus* genus in NP biodegradation. *Alicycliphilus denitrificans* BC and *A. denitrificans* K601^T have been reported to be able to degrade benzene and cyclohexanol, respectively, using different electron accepters (Mechichi et al., 2003; Weelink et al., 2008). Further purification will be needed to elucidate the roles of the specific bacteria in the biodegradation. In the initial stage of isolating the consortium capable of degrading NP, many types of bacteria might have attempted to adapt to the experimental conditions, and with time, only selected bacteria might have survived and degraded NP. The high efficiency and stability of NP-M2 in the process of NP biodegradation indicates that it is a promising candidate for NP bioremediation in the environment. Its application in environmental restoration in situ needs further investigation.

4. Conclusion

In this study, a facultative consortium, NP-M2, which could efficiently degrade NP by using it as the sole carbon source, was isolated. NP-M2 could rapidly degrade NP at concentrations ranging from 100 to 1000 mg/L, and removed 89.75% of 1000 mg/L NP within 8 days. In fact, 75.61% of the 1000 mg/L NP was eliminated within 48 h, indicating a degradation efficiency higher than that of other communities or pure bacterial strains. The addition of glucose and yeast extract improved the degradation efficiency to different degrees, with yeast extract yielding better results. Surface-active compounds excreted into the extracellular space might facilitate NP biodegradation. The biotoxicity assay showed a good detoxification of NP by NP-M2. The detection of intermediates and PCR analysis suggested that complete NP removal was initiated by the oxidation the aromatic ring, followed by step-wise degradation. The bacterial composition of the consortium was determined by 16S rDNA library analysis. NP-M2 was found to mainly comprise members of the *Sphingomonas*, *Pseudomonas*, *Alicycliphilus*, and *Acidovorax* genera, with the former two occupying 86.86% of the consortium. Our findings indicate that NP-M2 might represent an excellent tool for the bioremediation of environments contaminated with NP.

Acknowledgements:

This study was supported by the National Natural Science Foundation of China (41271335; 31470191), the Major State Basic Research Development Program of China (973 program) (2015CB150502).

Appendix A. Supplementary data

Supplementary data related to this article can be found at http://dx.doi.org/10.1016/j.envpol.2016.09.027.

References

Arslan, O.C., Parlak, H., 2007. Embryotoxic effects of nonylphenol and octylphenol in sea urchin *Arbacia lixula*. Ecotoxicology 16, 439–444.
Boitsov, S., Mjøs, S.A., Meier, S., 2007. Identification of estrogen-like alkylphenols in produced water from offshore oil installations. Mar. Environ. Res. 64, 651–665.
Brix, R., Hvidt, S., Carlsen, L., 2001. Solubility of nonylphenol and nonylphenol ethoxylates. On the possible role of micelles. Chemosphere 44, 759–763.
Buitrón, G., Torres-Bojorges, A.X., Cea-Barcia, G., 2015. Removal of p-nonylphenol isomers using nitrifying sludge in a membrane sequencing batch reactor. Chem. Eng. J. 281, 860–868.
Chakraborty, J., Dutta, T.K., 2006. Isolation of a *Pseudomonas* sp capable of utilizing 4-nonylphenol in the presence of phenol. J. Microbiol. Biotechnol. 16, 1740–1746.
Chang, B.V., Chiang, B.W., Yuan, S.Y., 2007. Biodegradation of nonylphenol in soil. Chemosphere 66, 1857–1862.
Chang, B.V., Liu, C.L., Yuan, S.Y., Cheng, C.Y., Ding, W.H., 2008. Biodegradation of nonylphenol in mangrove sediment. Int. Biodeterior. Biodegr. 61, 325–330.
Christiansen, T., Korsgaard, B., Jespersen, Å., 1998. Induction of vitellogenin synthesis by nonylphenol and 17β-estradiol and effects on the testicular structure in the eelpout *Zoarces viviparus*. Mar. Environ. Res. 46, 141–144.
Cladiere, M., Bonhomme, C., Vilmin, L., Gasperi, J., Flipo, N., Tassin, B., 2014. Modelling the fate of nonylphenolic compounds in the Seine River - part 1: determination of in-situ attenuation rate constants. Sci. Total Environ. 468, 1050–1058.
Conneely, A., Smyth, W., McMullan, G., 2001. Biodegradation of 4-nonylphenol by *Phanerochaete chrysosporium*. Abstr. General Meet. Am. Soc. Microbiol. 101, 621.
Corti, A., Frassinetti, S., Vallini, G., D'Antone, S., Fichi, C., Solaro, R., 1995. Biodegradation of nonionic surfactants. I. Biotransformation of 4-(1-nonyl) phenol by a Candida maltosa isolate. Environ. Pollut. 90, 83–87.
Corvini, P.F., Hollender, J., Ji, R., Schumacher, S., Prell, J., Hommes, G., Priefer, U., Vinken, R., Schaffer, A., 2006. The degradation of alpha-quaternary nonylphenol isomers by *Sphingomonas* sp. strain TTNP3 involves a type II ipso-substitution mechanism. Appl. Microbiol. Biotechnol. 70, 114–122.
Corvini, P.F.X., Vinken, R., Hommes, G., Schmidt, B., Dohmann, M., 2004. Degradation of the radioactive and non-labelled branched 4(3′,5'-dimethyl 3′-heptyl)-phenol nonylphenol isomer by *Sphingomonas* TTNP3. Biodegradation 15, 9–18.
Das, P., Mukherjee, S., Sen, R., 2008. Improved bioavailability and biodegradation of a model polyaromatic hydrocarbon by a biosurfactant producing bacterium of marine origin. Chemosphere 72, 1229–1234.

De Weert, J., Vinas, M., Grotenhuis, T., Rijnaarts, H., Langenhoff, A., 2010. Aerobic nonylphenol degradation and nitro-nonylphenol formation by microbial cultures from sediments. Appl. Microbiol. Biotechnol. 86, 761–771.
Deziel, E., Paquette, G., Villemur, R., Lepine, F., Bisaillon, J., 1996. Biosurfactant production by a soil *Pseudomonas* strain growing on polycyclic aromatic hydrocarbons. Appl. Environ. Microbiol. 62, 1908–1912.
Fuji, K., Urano, N., Ushio, H., Satomi, M., Iida, H., Ushio-Sata, N., Kimura, S., 2000. Profile of a nonylphenol-degrading microflora and its potential for bioremedial applications. J. Biochem. 128, 909–916.
Gabriel, F.L.P., Giger, W., Guenther, K., Kohler, H.-P.E., 2005. Differential degradation of nonylphenol isomers by *Sphingomonas xenophaga* Bayram. Appl. Environ. Microbiol. 71, 1123–1129.
Hao, R.-X., Zhang, Y., Lv, J., Zheng, X.-Y., 2010. Study on primary metabolites and possible biodegradation pathways of nonylphenol. Int. J. Environ. Pollut. 42, 136–147.
He, Z., Xiao, H., Tang, L., Min, H., Lu, Z., 2013. Biodegradation of di-n-butyl phthalate by a stable bacterial consortium, HD-1, enriched from activated sludge. Bioresour. Technol. 128, 526–532.
Huang, S.-L., Chen, H., Hu, A., Tuan, N.N., Yu, C.-P., 2014. Draft genome sequence of *Pseudomonas nitroreducens* strain TX1, which degrades nonionic surfactants and estrogen-like alkylphenols. Genome announc. 2.
Ieda, T., Horii, Y., Petrick, G., Yamashita, N., Ochiai, N., Kannan, K., 2005. Analysis of nonylphenol isomers in a technical mixture and in water by comprehensive two-dimensional gas chromatography-mass spectrometry. Environ. Sci. Technol. 39, 7202–7207.
Janicki, T., Krupiński, M., Długoński, J., 2016. Degradation and toxicity reduction of the endocrine disruptors nonylphenol, 4-tert-octylphenol and 4-cumylphenol by the non-ligninolytic fungus *Umbelopsis isabellina*. Bioresour. Technol. 200, 223–229.
Karci, A., Arslan-Alaton, I., Bekbolet, M., Ozhan, G., Alpertunga, B., 2014. H2O2/UV-C and Photo-Fenton treatment of a nonylphenol polyethoxylate in synthetic freshwater: follow-up of degradation products, acute toxicity and genotoxicity. Chem. Eng. J. 241, 43–51.
Kloos, K., Munch, J.C., Schloter, M., 2006. A new method for the detection of alkane-monooxygenase homologous genes (*alkB*) in soils based on PCR-hybridization. J. Microbiol. Meth. 66, 486–496.
Krupiński, M., Janicki, T., Pałecz, B., Długoński, J., 2014. Biodegradation and utilization of 4-n-nonylphenol by *Aspergillus versicolor* as a sole carbon and energy source. J. Hazard. Mater 280, 678–684.
Liu, X., Tani, A., Kimbara, K., Kawai, F., 2006. Metabolic pathway of xenoestrogenic short ethoxy chain-nonylphenol to nonylphenol by aerobic bacteria, *Ensifer* sp. strain AS08 and *Pseudomonas* sp. strain AS90. Appl. Microbiol. Biotechnol. 72, 552–559.
Lu, Z., Gan, J., 2014. Analysis, toxicity, occurrence and biodegradation of nonylphenol isomers: a review. Environ. Int. 73, 334–345.
Lu, Z., Reif, R., Gan, J., 2015. Isomer-specific biodegradation of nonylphenol in an activated sludge bioreactor and structure–biodegradability relationship. Water Res. 68, 282–290.
Mechichi, T., Stackebrandt, E., Fuchs, G., 2003. *Alicycliphilus denitrificans* gen. nov., sp. nov., a cyclohexanol-degrading, nitrate-reducing β-proteobacterium. Int. J. Syst. Evol. Microbiol. 53, 147–152.
Neamţu, M., Frimmel, F.H., 2006. Photodegradation of endocrine disrupting chemical nonylphenol by simulated solar UV-irradiation. Sci. Total Environ. 369, 295–306.
Pérez-de-Mora, A., Engel, M., Schloter, M., 2011. Abundance and diversity of n-alkane-degrading bacteria in a forest soil co-contaminated with hydrocarbons and metals: a molecular study on *alkB* homologous genes. Microb. Ecol. 62, 959–972.
PengFei, S., LiLing, L., Guan, W., YuHua, Z., 2013. Isolation and algicidal characteristics of *Citrobacter* sp. strain N10. J. Zhejiang Univ. Agric. Life Sci. 39, 613–620.
Pickford, K.A., Thomas-Jones, R.E., Wheals, B., Tyler, C.R., Sumpter, J.P., 2003. Route of exposure affects the oestrogenic response of fish to 4-tert-nonylphenol. Aquat. Toxicol. 65, 267–279.
Porter, A.W., Hay, A.G., 2007. Identification of opdA, a gene involved in biodegradation of the endocrine disrupter octylphenol. Appl. Environ. Microbiol. 73, 7373–7379.
Press-Kristensen, K., Lindblom, E., Schmidt, J.E., Henze, M., 2008. Examining the biodegradation of endocrine disrupting bisphenol A and nonylphenol in WWTPs. Water Sci. Technol. 57, 1253–1256.
Preuss, T.G., Gehrhardt, J., Schirmer, K., Coors, A., Rubach, M., Russ, A., Jones, P.D., Giesy, J.P., Ratte, H.T., 2006. Nonylphenol isomers differ in estrogenic activity. Environ. Sci. Technol. 40, 5147–5153.
Różalska, S., Soboń, A., Pawłowska, J., Wrzosek, M., Długoński, J., 2015. Biodegradation of nonylphenol by a novel entomopathogenic *Metarhizium robertsii* strain. Bioresour. Technol. 191, 166–172.
Rocha, M.J., Cruzeiro, C., Reis, M., Rocha, E., Pardal, M.A., 2013. Determination of 17 endocrine disruptor compounds and their spatial and seasonal distribution in the Sado River Estuary (Portugal). Toxicol. Environ. Chem. 95, 237–253.
Różalska, S., Pawłowska, J., Wrzosek, M., Tkaczuk, C., Długoński, J., 2013. Utilization of 4-*n*-nonylphenol by *Metarhizium* sp. isolates. Acta Biochim. Pol. 60, 677–682.
Shanthanagouda, A.H., Patil, J.G., Nugegoda, D., 2013. Effects of exposure to oestrogenic compounds on aromatase gene expression are gender dependent in the rainbowfish, *Melanotaenia fluviatilis*. Comp. Biochem. Phys. C 157, 162–171.
Singh, A., Van Hamme, J.D., Ward, O.P., 2007. Surfactants in microbiology and biotechnology: Part 2. Application aspects. Biotechnol. Adv. 25, 99–121.
Soares, A., Guieysse, B., Delgado, O., Mattiasson, B., 2003a. Aerobic biodegradation of nonylphenol by cold-adapted bacteria. Biotechnol. Lett. 25, 731–738.
Soares, A., Guieysse, B., Mattiasson, B., 2003b. Biodegradation of nonylphenol in a continuous packed-bed bioreactor. Biotechnol. Lett. 25, 927–933.
Sun, P., Hui, C., Wang, S., Khan, R.A., Zhang, Q., Zhao, Y.-H., 2016. Enhancement of algicidal properties of immobilized *Bacillus methylotrophicus* ZJU by coating with magnetic Fe_3O_4 nanoparticles and wheat bran. J. Hazard. Mater 301, 65–73.
Tanghe, T., Dhooge, W., Verstraete, W., 2000. Formation of the metabolic intermediate 2, 4, 4-trimethyl-2-pentanol during incubation of a shape *Sphingomonas* sp. strain with the xeno-estrogenic octylphenol. Biodegradation 11, 11–19.
Tuan, N.N., Hsieh, H.-C., Lin, Y.-W., Huang, S.-L., 2011. Analysis of bacterial degradation pathways for long-chain alkylphenols involving phenol hydroxylase, alkylphenol monooxygenase and catechol dioxygenase genes. Bioresour. Technol. 102, 4232–4240.
Viñas, M., Sabaté, J., Espuny, M.J., Solanas, A.M., 2005. Bacterial community dynamics and polycyclic aromatic hydrocarbon degradation during bioremediation of heavily creosote-contaminated soil. Appl. Environ. Microbiol. 71, 7008–7018.
Wang, Z., Dai, Y., Zhao, Q., Li, N.N., Zhou, Q.H., Xie, S.G., 2015a. Nonylphenol biodegradation, functional gene abundance and bacterial community in bioaugmented sediment: effect of external carbon source. Environ. Sci. Pollut. Res. 22, 12083–12091.
Wang, Z., Yang, Y., Dai, Y., Xie, S., 2015b. Anaerobic biodegradation of nonylphenol in river sediment under nitrate- or sulfate-reducing conditions and associated bacterial community. J. Hazard. Mater 286, 306–314.
Wang, Z., Yang, Y., Sun, W., Xie, S., 2014. Biodegradation of nonylphenol by two alphaproteobacterial strains in liquid culture and sediment microcosm. Int. Biodeterior. Biodegrad. 92, 1–5.
Watanabe, W., Hori, Y., Nishimura, S., Takagi, A., Kikuchi, M., Sawai, J., 2012. Bacterial degradation and reduction in the estrogen activity of 4-nonylphenol. Biocontrol Sci. 17, 143–147.
Weelink, S.A., Tan, N.C., ten Broeke, H., van den Kieboom, C., van Doesburg, W., Langenhoff, A.A., Gerritse, J., Junca, H., Stams, A.J., 2008. Isolation and characterization of *Alicycliphilus denitrificans* strain BC, which grows on benzene with chlorate as the electron acceptor. Appl. Environ. Microbiol. 74, 6672–6681.
Whang, L.-M., Liu, P.-W.G., Ma, C.-C., Cheng, S.-S., 2009. Application of rhamnolipid and surfactin for enhanced diesel biodegradation—Effects of pH and ammonium addition. J. Hazard. Mater 164, 1045–1050.
Wheeler, T.F., Heim, J.R., LaTorre, M.R., Janes, A.B., 1997. Mass spectral characterization of *p*-nonylphenol isomers using high-resolution capillary GC-MS. J. Chromatogr. Sci. 35, 19–30.
Wu, F.F., Qiu, L.F., 2011. Kinetic study on the biodegradation of nonylphenol by *Rhodotorula* sp, advanced materials research. Trans. Tech. Publ. 575–578.
Wu, Z.-y., Zeng, Z.-d., Marriott, P.J., 2010. Comparative qualitative analysis of nonylphenol isomers by gas chromatography–mass spectrometry combined with chemometric resolution. J. Chromatogr. A 1217, 7759–7766.
Yuan, S.Y., Yu, C.H., Chang, B.V., 2004. Biodegradation of nonylphenol in river sediment. Environ. Pollut. 127, 425–430.
Zhang, L., Cao, Y., Hao, X., Zhang, Y., Liu, J., 2015. Application of the GREAT-ER model for environmental risk assessment of nonylphenol and nonylphenol ethoxylates in China. Environ. Sci. Pollut. Res. 22, 18531–18540.
Zhang, Y., Maier, W.J., Miller, R.M., 1997. Effect of rhamnolipids on the dissolution, bioavailability, and biodegradation of phenanthrene. Environ. Sci. Technol. 31, 2211–2217.